Boson peak in confined disordered systems

Reiner Zorn
IFF, Forschungszentrum Jülich, D-52425 Jülich, Germany
(Received 1 February 2010; published 26 February 2010)

The vibrational density of states (VDOS) of disordered systems shows a low-frequency excess, the so-called boson peak. Experiments show a change in the shape of the boson peak when the systems are spatially confined. Depending on the type of confinement (hard or soft) the low-frequency wing of the boson peak is either suppressed or enhanced. Here, a simple model, a crystalline system with disordered nearest-neighbor force constants, is studied with boundary conditions mimicking the confinement. The VDOS calculated by numerical diagonalization shows qualitatively the same confinement effect as the experiment. In this model, the effect is a consequence of modes of the bulk system being shifted up or down for hard and soft confinement, respectively. A simple rescaling procedure is suggested to convert the VDOS of the bulk into that of the confined system.

DOI: 10.1103/PhysRevB.81.054208 PACS number(s): 63.50.−x, 61.43.Fs, 63.22.Kn

I. INTRODUCTION

A ubiquitous feature of the vibrational density of states (VDOS) $g(\omega)$ in amorphous materials is the occurrence of low-frequency vibrations, which are not present in the crystalline counterparts.[1] It was first detected indirectly as an anomaly in the low-temperature specific heat[2] and by Raman spectroscopy,[3] later also by inelastic neutron scattering (INS),[4] and nuclear inelastic scattering/absorption (NIS/NIA).[5] The latter methods provide $g(\omega)$ directly and it turns out that it shows an extra contribution with respect to the Debye VDOS $g_{\mathrm{Debye}}(\omega) \propto \omega^2$. In other words, the reduced VDOS, $g(\omega)/\omega^2$, is not constant but shows a peak a low frequency, which is commonly called "boson peak" (BP).

There are currently several competing explanations of the BP phenomenon, which can be roughly classified in two categories: (i) the modes constituting the BP are distinct from sound waves and arise from peculiarities of the interatomic forces in amorphous materials, e.g., soft potentials.[6,7] (ii) The VDOS of the amorphous system is just a modification of the crystalline VDOS due to the fluctuation of force constants.[8] In the latter picture, the BP would "only" be the broadened version of the lowest van Hove singularity in the corresponding crystalline system.[9]

Recent INS experiments showed that there is a characteristic effect on the BP if molecular liquids or polymers are confined in nanoporous silica with pore diameters in the range 25–200 Å (Refs. 10 and 11): the low-frequency wing of the BP is suppressed while the high frequency wing is nearly unchanged. In consequence, the BP seems to become sharper and shifted toward higher frequency. This effect could also be confirmed by NIA.[12]

In many studies of dynamics of glass-formers in confinement, there was the indication that surface effects play an important role in addition to the bare confinement (size) effect.[13] In most cases, the confinement used was "hard" in the sense that the dynamics of the confining matrix was slower than that of the confined material. This motivated experiments exploring the opposite situation of "soft" confinement. This situation could be realized by enclosure of a glass-forming liquid in microemulsion droplets.[14] When the VDOS of this soft-confined system was studied,[15] it turned out that the effect on the BP is opposite: the VDOS below the BP maximum increases and the BP seems to be completely washed out.

Although these experiments are in some aspects still preliminary, they indicate that the BP depends strongly on the boundary conditions of the confined glass-former. Therefore, it is interesting to study this effect in a computational model system where the boundary conditions can be chosen at will. Here, the probably simplest system showing a BP anomaly in the VDOS was used, the force-constant-disordered lattice.[9,16] This model is based on the calculation of the vibrational spectrum of a system of "atoms" located on an ideal crystalline lattice, i.e., no structural disorder of the atoms is assumed.

In the last decade, considerable activity has been invested in the simulation of more realistic model exhibiting a BP. This was done for model potentials (e.g., soft spheres, Lennard-Jones)[17,18] as well as for realistic potentials of glass-forming materials (e.g., silicon, silica).[19–21] It turns out that certain properties of the vibrational spectrum can only be mimicked by realistic models presumably because they contain positional disorder in addition to force-constant disorder.[22] Nevertheless, this study will use the extremely simplified disordered force-constant model because it is already able to produce the basic feature to be studied here, the boson peak.

In Sec. II, the disordered force-constant model will be briefly recalled and its modification to represent the confined situation will be described. Numerical results will be presented in Sec. III for different confinement sizes and geometries. It will be shown that a simple rescaling relation allows to convert the VDOS of the bulk to that of the confined system (Sec. IV). The rescaling relation will be tested on experimental data from inelastic neutron scattering too. Finally, the consequences for the understanding of the BP will be discussed.

II. DISORDERED FORCE-CONSTANT MODEL

The probably simplest systems showing a boson peak anomaly are derived from the model of a crystal introducing

a disorder in the force constants between the atoms. Harmonic forces are assumed between neighboring atoms with a random distribution of force-constants K_{ij}. Such models do not include any positional disorder of the atoms as, e.g., models based on quenched molecular dynamics[17–21] do. In addition to their simplicity, these models have the advantage that the coherent potential approximation (CPA) works very well for infinite systems and reproduces the numerical results accurately.[9,16] Here, the problem is that for the confined systems, the structure is not translationally invariant, especially boundary atoms do not have the same number of nearest neighbors. Translational invariance is a prerequisite of the currently applied CPA calculations. An extension of CPA to finite systems may be possible but is beyond the scope of this article.

The systems considered here are generated mostly the same way as those in Ref. 16: a simple-cubic lattice is used. The displacement of the atoms is taken as a scalar variable.[23] A Gaussian distribution of force constants with a width $\sigma=1$ around the average force-constant $K_0=1$ truncated at $K_{\min}=-0.2$ is used. The only difference introduced here concerns the force constants at the boundary for the "confined" systems. For the "soft confinement," open boundary conditions are imposed by setting the boundary force constants to zero. To simulate a hard confinement, the energy terms at the boundaries are replaced like $K_L(r_L-r_0)^2/2$ by $K_L r_L^2$. This has the meaning of a boundary spring with a double average strength connected to a wall. It is clear that by this modification, the zero-frequency mode corresponding to translation of the whole system vanishes. The *double* force constant is introduced because for this choice some of the eigenmodes of the ordered periodic boundary conditions (PBC) system are also eigenmodes of the ordered confined system. All masses are assumed to be equal, $m=1$.

$L\times L\times L$ systems are studied where $L\leq 23$ due to memory limitation of the Hamiltonian matrix. The eigenvalues of the Hamiltonian matrix were calculated by the routine DSYEV from the LAPACK library. For some systems, also the eigenvectors were calculated in order to evaluate the sound velocities and participation ratios. To see the influence of system size on the confinement effect and possible finite-size effects, two system sizes are compared. For $L=15,90$ repetitions with different random seeds are carried out to improve statistics, for $L=23,25$ repetitions. From the eigenvalues, the reduced VDOS $g(\omega)/\omega^2$ is calculated using a modified histogram analysis. It is assumed that $g(\omega)/\omega^2$ is constant over a certain interval and its value is determined by the condition that the integral over that interval results in the number of eigenfrequencies actually counted. The interval widths are chosen such that the same number of eigenfrequencies falls into each of them. To illustrate this implied meaning of the $g(\omega)/\omega^2$ values, the histogram is displayed for one calculation in Fig. 1. It can be seen that the procedure leads to a rather smooth histogram for the given repetition counts and sufficiently small interval numbers (50 for $L=15$ and 75 for $L=23$). For all other calculations, only $g(\omega)/\omega^2$ vs the average ω in the histogram interval is shown as points.

It has to be mentioned that the occurrence of negative eigenvalues cannot be completely avoided for the systems constructed as described above. Table I shows the number of

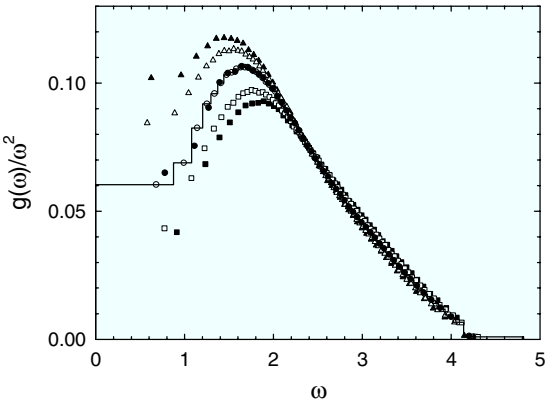

FIG. 1. Comparison of the reduced VDOS for systems with different boundary conditions (model with one force-constant distribution). Circles correspond to periodic boundary conditions (PBC), triangles to boundary conditions corresponding to hard confinement, and squares to open boundary conditions, viz. soft confinement. Filled symbols correspond to a system-size $L=15$ and open symbols to $L=23$. For $L=23$ with PBC, the underlying histogram is shown.

systems with negative eigenvalues and the number of negative eigenvalues resulting from the numerical diagonalisation. It can be seen that the generated systems rarely contain negative eigenvalues. In most of the cases where negative eigenvalues occur, there is only one of these per system. In the calculation of the histograms presented here the negative eigenvalues were not considered. This means that, strictly speaking, the normalization condition of the VDOS $\int g(\omega)\mathrm{d}\omega=1$ is not fulfilled. But from the fact that in the worst case among 377 300 eigenvalues studied there, were 22 negative the deficiency in the integral can be estimated to be $<10^{-4}$. This situation occurred only for one system type ($L=7$ with open boundary conditions), for all others, the frequency of negative eigenvalues was an order of magnitude less. It was also tested whether those (up to 8%) systems, which have (in most cases single) negative eigenvalues lead to a different $g(\omega)$. No statistically significant difference was found. So the same histogram curves would be obtained if the systems with negative eigenvalues were excluded from the statistics. Nevertheless, in order to avoid a hidden statistical bias, this was not done. Alternative distributions of force constants as full Gaussian or box distribution were checked. But in the end, the truncated Gaussian was the best compromise to avoid negative eigenvalues while retaining a VDOS showing a pronounced BP.

III. NUMERICAL RESULTS

As Fig. 1 shows, for the PBC system, there is only a small difference between $L=15$ and $L=23$ indicating that finite-size effects can be neglected. Therefore, the PBC result of the larger ($L=23$) system has been taken as representative for an infinite system.

The systems with hard and soft confinement show significant deviations from the PBC (bulk) system. The low-frequency limit of $g(\omega)/\omega^2$ is decreased or increased, the BP

TABLE I. Number of systems with negative eigenvalues and the number of negative eigenvalues for all systems of one type.

L	Confinement type	Systems	Systems with negative eigenvalues	Eigenvalues of all generated systems	Negative eigenvalues
23	−(PBC)	25	1	304175	1
23	Hard	25	1	304175	1
23	Soft	25	2	304175	2
15	−(PBC)	90	0	303750	0
15	Hard	90	0	303750	0
15	Soft	90	1	303750	1
7	−(PBC)	1100	0	377300	0
7	Hard	1100	0	377300	0
7	Soft	1100	22	377300	22
15	1D, hard	90	0	303750	0
15	1D, soft	90	1	303750	1
15	2D, hard	90	1	303750	1
15	2D, soft	90	3	303750	4
15	1D, mixed	90	2	303750	2

shifted to higher or lower frequencies, respectively. This is exactly the qualitative behavior found in the experiment.[10,25] As expected, the differences to the bulk result reduce for increasing system size.

In retrospect, an unmentioned difference in the low-frequency VDOS of early models of vitreous silicalike compounds between fixed (hard) and free (soft) boundary conditions[24] can be presumed the same phenomenon. But due to size limitations and the impossibility to realize PBC in this model, a comparison with the undistorted BP is not possible.

For an infinite system, one would expect the VDOS at low frequencies (i.e., significantly lower than the BP maximum) to be related to the sound velocity by the relation from the Debye model,

$$g(\omega) = \frac{\rho}{2\pi^2 v^3}\omega^2. \tag{1}$$

Setting the lattice constant $a=1$ in addition to $m=1$, one obtains $g(\omega)/\omega^2 = 1/2\pi^2$ for the ordered model with $K_{ij}=1$. For the ordered model, the VDOS can be calculated analytically[16] and it shows this limit. To check the low-frequency limit here, the sound velocity is calculated in two ways: (i) the lowest eigenvectors are calculated. These represent nearly unperturbed plane waves with the mode indices (1,0,0), (1/2,1/2,1/2), and (1/2,0,0) for the PBC, hard-confined, and soft-confined systems, respectively. The sound velocity can then be calculated from the relation $v=\omega/q$ where $q=2\pi L^{-1}$, $\sqrt{3}\pi L^{-1}$, and πL^{-1} for the three system types. The disadvantage of this method is that the calculated sound velocity is not exactly the one in the limit $q\to 0$. Due to the dispersion, it will be slightly lower. (ii) Following a suggestion by Léonforte,[20] the elastic modulus of the system can be calculated for the PBC system: for a system in which the bounding box size $A=L\cdot a$ is reduced in one dimension by ΔA, the new equilibrium positions of the atoms are calculated. It has to be noted that these positions are not just the affinely rescaled original positions.[20] The atoms may rearrange lowering the energy. The potential energy U of the "compressed" system is then calculated and from this the elastic modulus by $M=2U/\Delta A^2 A$. The disadvantage here is that there is no obvious way to apply this procedure to the confined system without tampering with the boundary conditions.

Table II shows the results of these sound velocity calculations. As expected, the sound velocity from low-frequency modes is slightly lower. It turns out that for both calculation methods, there is a distribution of sound velocities. This can be clearly seen from the fact that the variance does not increase with the number of calculated realizations with $\sqrt{N}$ but levels off to the presented values at system numbers around those listed in Table I. For the calculation from low q, this distribution can be related to the broadening of neutron and x-ray Brillouin scattering lines in disordered systems.[26] But currently, the statistics of the data is not sufficient to allow a quantitative statement about questions as, e.g., the exponent

TABLE II. Sound velocities of selected systems. $v(q_{\min})$ is the value calculated from the lowest eigenvalues corresponding to the minimal wave vector allowed by the confinement type. $v(0)$ is the sound velocity calculated via the elastic modulus as described in Ref. 20. Note that the variation $\pm\ldots$ is *not* a statistical error but reflects the distribution of sound velocities in multiple instances of the systems.

L	Confinement type	$q_{\min}$	$v(q_{\min})$	$v(0)$
23	−(PBC)	0.27	1.0016 ± 0.0053	1.0070 ± 0.0036
15	−(PBC)	0.42	1.0016 ± 0.0053	1.0070 ± 0.0036
15	Hard	0.36	1.0081 ± 0.0028	
15	Soft	0.21	1.0013 ± 0.0051	

of the relation between width and frequency of the Brillouin line.

All sound velocities do not differ much from that of the ordered model with $K_{ij}=1$, which is $v_{\text{ordered}}=1$. Of course, this is an accidental property of the distribution chosen here. Nevertheless, one would then expect all curves in Fig. 1 to show the same low-frequency limit, ≈ 0.05. That this is not the case has two reasons: (i) even in the PBC system, there is a deviation because the upper boundary of the lowest histogram bin is chosen rather high. In the range of this first bin, the VDOS is already increasing noticeably above the Debye limit. On the other hand, this bin cannot be chosen slimmer because it has to include several soundlike modes to produce a smooth average. (ii) In the case of confined systems, the deviation is bigger, positive for the soft confinement and negative for the hard. Here, the assumption of the Debye model (1) that the density of modes in q space is homogeneous is not fulfilled. For low q, it has to be taken into account that certain modes are not possible for hard confinement and certain modes are more "crowded" for the soft confinement. A visual inspection of modes in the low-frequency range showed no indication of non-sound-wave modes contributing to the discrepancy between Debye VDOS and that calculated except for some spurious modes whose number is similarly small as that of negative eigenvalues.

It is sometimes argued that the simple-cubic system with scalar vibrations is unphysical for two reasons: (i) the simple-cubic system is mechanically unstable, more precisely, shows of the order of L^2 zero-frequency eigenmodes. This would be true if the model were realized as a three-dimensional bead-and-spring model. In this case, the vibration amplitude is a three-dimensional vector. Of the three components of the amplitude, only the one parallel to the distance vector to the nearest neighbor is coupled in first order. On the contrary, for the model considered here, all amplitudes are coupled between neighbors. Therefore, there is only one zero-frequency mode, which corresponds to translation of the whole system. Converting this to a mechanical model, this would be a model with springs, which are equally stiff with respect to bending as with respect to stretching. This immediately leads to a second objection.

(ii) Even if one considers the atoms in the model as coarse-grained entities representing small "blocks" of actual matter, one would expect the compliance to shear to be lower than that to compression. In other words, one would expect a difference between transverse and longitudinal modes. This can be implemented in the model by multiplying the random force constants in one spatial direction by a factor. (According to the empirical relation that the longitudinal sound velocity is usually about twice the transverse, the factor was chosen to be 4.) Again, it can be argued that for the three-dimensional system this has to be done for all three components of the amplitude but on the simple-cubic grid the Hamiltonian matrix decomposes into three independent ones. Therefore, also here the, scalar treatment cannot be improved.

Figure 2 shows the reduced VDOS calculated for this modification. It can be seen that the general effects of the hard and soft confinement are the same as in the case where

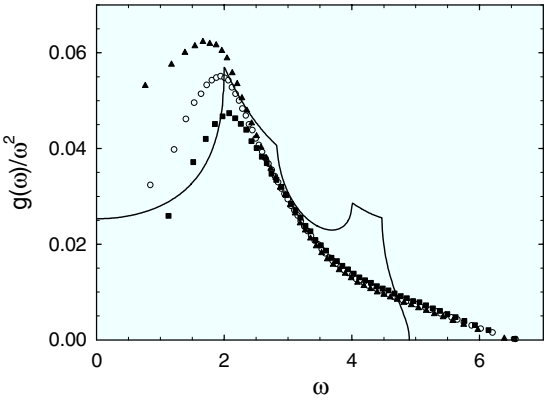

FIG. 2. Comparison of the reduced VDOS for systems with different boundary conditions for a model with different longitudinal and transverse force-constant distributions, $\overline{K_{\text{L}}}=4\overline{K_{\text{T}}}$. Circles correspond to periodic boundary conditions, triangles to boundary conditions corresponding to hard confinement, and squares to open boundary conditions, viz. soft confinement. Filled symbols correspond to a system-size $L=15$ and open symbols to $L=23$. The continuous curve is the analytical result for the corresponding ordered system

no distinction between transverse and longitudinal force constants was made. The comparison with the analytically calculated VDOS of the ordered system also shows that the BP is related to the lower van Hove singularity *of the transverse mode*.

In experiments, amorphous materials are often confined only with respect to a limited number of spatial dimension, e.g., in one dimension as polymer films.[27] Therefore, it is interesting to check what the effect on the BP is for the model systems studied here if only one or two Cartesian direction have hard/soft boundary conditions but the others are still periodic. The result is shown in Fig. 3 for hard confinement. As one would naïvely expect, the results lie in between the fully confined and the PBC system. Therefore, for experiments on free-standing films one would expect a similar but weaker effect on the BP as for three-dimensional soft confinement. This was not observed in the only inelastic neutron scattering experiment on free-standing polymer films.[28] But it has to be noted that these experiments were done on 55–107 nm thick films. This size is much larger than the usual size of the three-dimensional confinement in studies of molecular liquids (2.5–20 nm). Considering the $1/L$ scaling motivated in the next section, the effect may have been too small to be observed.

Finally, a common experimental situation is that of a supported film,[29] i.e., a film with hard confinement on one side and a free surface on the other. As Fig. 4 shows, the model yields an exact compensation of the effects of the two surfaces here. The only existing experimental determination of the VDOS in this geometry[30] shows an unchanged BP shape in agreement with this result but a reduced overall intensity in contrast. Also in this study, the film thickness was comparatively large (40–100 nm).

A crucial question in the study of vibrational states in disordered systems is that of *localization*.[31,32] There are different approaches to quantify localization. Of these, two will

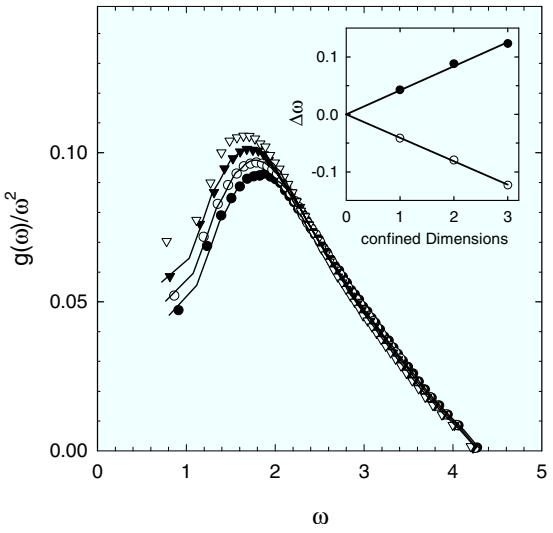

FIG. 3. Reduced VDOS for systems confined in selected dimensions only. The symbols represent hard-confined $L=15$ systems: 3D-cube (filled circles), 2D-wire (open circles), 1D-plate (filled triangles). For comparison, also the unconfined system is shown (open triangles). The lines represent the VDOS of the PBC system with $L=23$ rescaled by Eqs. (6) and (5) (see Sec. IV). The inset shows a plot of $\Delta\omega$ from rescaling fits. Filled symbols correspond to hard confinement and empty symbols to soft confinement. The lines are fits of proportionalities to the number of confined dimensions.

be used here to check for possible differences due to different boundary conditions: level distance statistics[16] and participation ratio.[31]

The procedure to obtain the level distance statistics is basically the same as in Ref. 16. The eigenfrequencies ω_j are converted into normalized levels ϵ_j, which have a uniform density 1 between 0 and L^3. The number of states up to frequency ω is

$$G(\omega) = L^3 \int_0^\omega g(\omega')\mathrm{d}\omega'. \tag{2}$$

By mapping the eigenvalues through $\epsilon_j = G(\omega_j)$, the desired uniformity is achieved. For $g(\omega)$ in Eq. (2), histograms as in

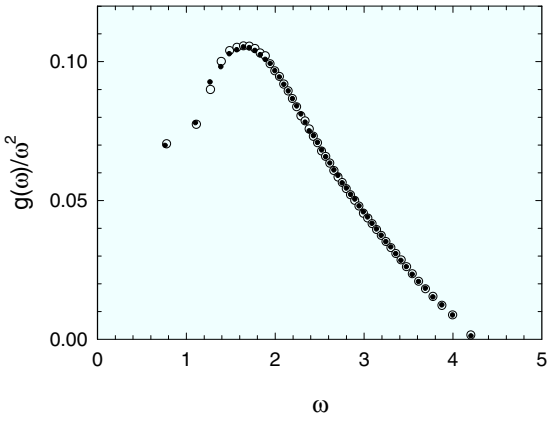

FIG. 4. Reduced VDOS of system confined in one dimension by mixed boundary conditions (small filled symbols) compared to periodic boundary conditions (large open symbols).

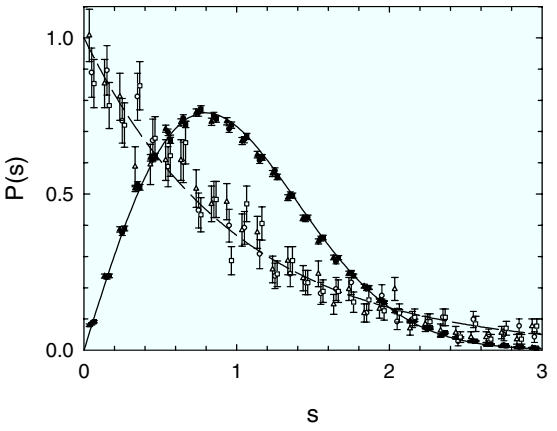

FIG. 5. Level distance statistics for the eigenvalues close to the BP ($\omega=1.2,\ldots,2$, filled symbols) and for the 0.5% highest eigenvalues (hollow symbols). Circles, triangles, and squares correspond to PBC, hard confinement, and soft confinement, respectively. System-size $L=15$. (For reasons of clarity, the ω values are slightly offset.) The lines represent the Gaussian othogonal ensemble (GOE) (continuous) and Poisson statistics (dashed).

Fig. 1 are used but with an increased bin resolution in the high frequency region. Then, a histogram of the distances $s_j = |\epsilon_{j+1} - \epsilon_j|$ is constructed. The results are shown in Fig. 5 together with the distribution of the Gaussian orthogonal ensemble (GOE), $P(s) = \frac{1}{2}\pi s \exp(-\pi s^2/4)$, expected for delocalized states because of level repulsion, and the Poisson distribution, $P(s) = \exp(-s)$, expected for localized states. It can be seen that in the BP region ($\omega=1.2,\ldots,2$) irrespective of the nature of the boundary conditions the states follow the expected behavior for delocalized modes. This turns out to be the same for different choices of the analyzed interval between $\omega=1$ and $\omega=4$. Only for the highest 0.5% modes (i.e., at $\omega>4.21,\ldots,4.33$ depending on the boundary condition type), the statistics becomes clearly Poissonian. Already by including the next lower 0.5%, significant deviations from Poissonian statistics are generated. The modes below $\omega=1$ are difficult to analyze because the spectrum disintegrates into bunches of near-sound-wave modes there, so no clear statement can be made here. In summary, as found for the PBC system in Ref. 16, there is no indication of localization except for the band edge for all types of boundary conditions.

Because in the calculation performed here, also the eigenvectors are obtainable, as a direct measure of localization, the participation ratio can be calculated

$$p_j = \left(L^3 \sum_{l=1}^{L^3} {e_{jl}}^4 \right)^{-1}. \tag{3}$$

Here, j counts the modes and l the lattice sites, and e_{jl} for $j=1,\ldots,L^3$ are the eigenvectors. In the ideal case of equal amplitudes (which is only realized for the $\omega=0$ translational mode), one obtains $p=1$. For localized modes, the value should be significantly smaller. But it has to be noted that even for sound waves, the value of one will not be attained. There will be a spread of the amplitudes between nodes and

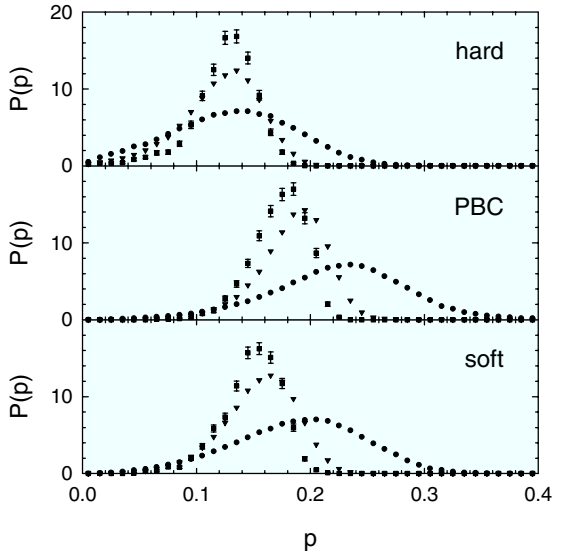

FIG. 6. Statistics of the participation ratio in the BP range ($\omega = 1.2, \ldots, 2$). Circles, triangles, and squares represent different system-sizes $L=7$, 15, and 23, respectively. (Error bars are drawn only for $L=23$, for the other systems they would be smaller than the symbol size.)

maxima leading to $p \approx 0.1, \ldots, 0.7$. What is more characteristic is that p scales with the system size as L^{-3} for localized modes. For reasons of computing time, this calculation was only done for one instance of the $L=23$ system, for the other system sizes as noted in Table I. Therefore, the statistics for $L=23$ is not as good as for the smaller systems. The participation ratios were evaluated by histograms in the same ω regions as before for the level distance statistics.

The result for the BP region is shown in Fig. 6. The values are smaller than one but it is clear that there is no scaling with the system size, which would be $7^{-3}:15^{-3}:23^{-3}$. For hard boundary conditions, the average participation ratio is smaller. This is not surprising because these boundary conditions enforce nodes at the boundary concentrating the amplitude into the center of the system. A similar but smaller effect can be seen for soft boundary conditions where the maxima of the amplitudes are forced to the boundary. Notably, the distribution of participation ratios is not unchanged between $L=15$ and $L=23$. This shows that concerning this quantity there is still some finite-size effect remaining in contrast to $g(\omega)$.

Figure 7 shows the statistics of the participation ratio for the 0.5% highest modes. On an absolute scale the values are a magnitude smaller than in the BP region. What is more important is that in the high frequency region there is a big influence of system size. As the insets in the figure show the expected scaling with L^{-3} is fulfilled even quantitatively. So also from the criterion of participation ratio, the high frequency modes are localized.

In summary, both ways to analyze the degree of localization show no difference between confined and PBC system. In all cases, localized modes can be confirmed only at the band edge. As pointed out by Schober, it may be unjustified to use the modes from the numerical diagonalisation directly in such evaluations.[17,31] There, it is shown that by rotating

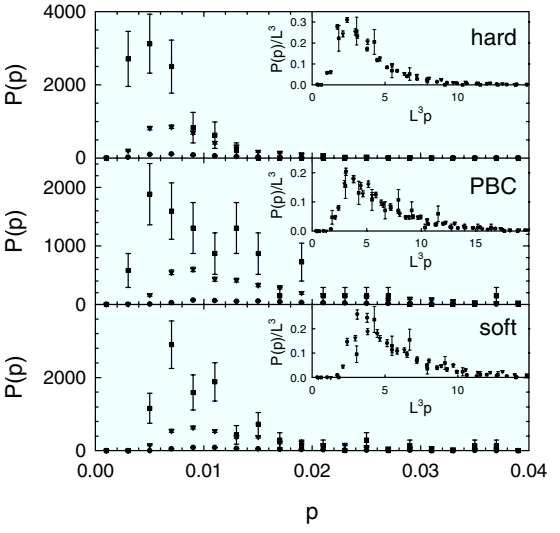

FIG. 7. Statistics of the participation ratio for the 0.5% highest modes. Circles, triangles, and squares represent different system-sizes $L=7$, 15, and 23, respectively. The inset shows tests of the scaling with system size expected for localized modes.

the basis of modes in a narrow energy range one can decompose the directly obtained modes into extended and localized ones. It is probably possible to do this with the modes obtained here, too, but this would go beyond the scope of the current publication and probably also not lead to differences between the boundary condition types because there are no differences in the primary data.

IV. BULK-TO-CONFINED RESCALING

A. Rescaling formula

Figure 8 shows the change in eigenfrequencies for one particular $L=15$ system induced by changing the boundary conditions. It can be seen that the majority of eigenfrequen-

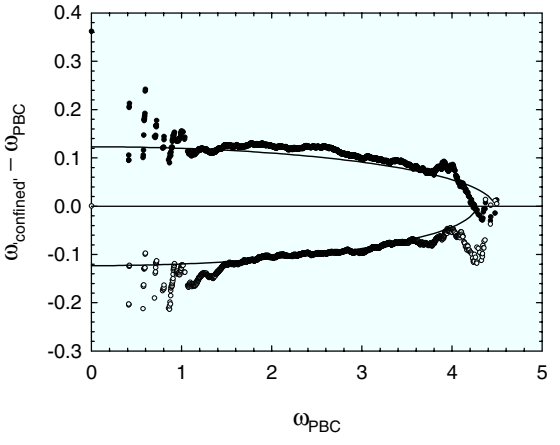

FIG. 8. Eigenfrequency difference induced by change in the boundary conditions. The symbols show the difference of the eigenfrequencies between an $L=15$ system with confinement boundary conditions (hard: filled symbols, soft: empty symbols) and periodic boundary conditions. The curves represent the difference expected from Eq. (5).

cies increases for the transition PBC-hard and decreases for PBC-soft. In this comparison, the modes are naïvely ordered by the magnitude of the eigenfrequency. Of course, this is debatable since the modes compared may not be the "same" in the sense of an identical wave vector. (A wave vector is not defined in the disordered system.)

Therefore, it makes sense to consider the situation in the corresponding systems without force-constant disorder briefly. For these systems, there is an exact rule telling which mode evolves into which upon changing the boundary conditions: all mode eigenvectors of the ordered PBC system can be written as

$$u(l_1,l_2,l_3) = \prod_{\alpha=1}^{3} \mathrm{trig}\left(\frac{2\pi k_\alpha (l_\alpha + 1/2)}{L}\right), \tag{4}$$

where (k_1,k_2,k_3) with $k_\alpha = 0,1,\ldots,(L-1)/2$ (assuming odd L) is the mode multi-index, (l_1,l_2,l_3) with $l_\alpha = 0,1,\ldots,L-1$ determines the position in the lattice, and each function "trig" may either be "cos" or "sin."[33] The choice of $\cos(x+\pi/L)$ and $\sin(x+\pi/L)$ for the base vectors instead of $\exp(\mathrm{i}x)$ and $\exp(-\mathrm{i}x)$ leads to the fact that expression (4) describes the eigenvectors in the hard- and the soft-confined ordered system too, except for the restriction that only pure sine modes are allowed for the hard confinement and only pure cosine modes for the soft. On the other hand, for the latter systems also half-integral values for k_α are allowed, namely, $k_\alpha = 0,1/2,1,\ldots,(L-1)/2$ for the soft and $k_\alpha = 1/2,1,\ldots,L/2$ for the hard. It can be easily seen that if a mode exists with the same combination of trigonometric functions in the PBC *and* the confined system, it remains unchanged upon changing the boundary conditions. Otherwise, in the hard-confined system, the mode multiindex changes such that a cosine changes into a sine and the k_α in its argument is *increased* by 1/2. Correspondingly for the soft-confined system, sines are changed into cosines and the affected k_α are *reduced* by 1/2.

Because (k_1,k_2,k_3) is related to the wave number by $q = (2\pi/La)\sqrt{k_1^2+k_2^2+k_3^2}$ (a being the lattice constant), this leads to a reduction of q in the case of soft confinement and an increase for hard confinement. In consequence, the eigenfrequency is reduced in the former case and augmented in the latter. To derive a simple approximate rescaling relation between the eigenfrequencies in the PBC and confined situations, it is assumed that all modes are shifted by the same amount Δq. Furthermore, instead of using the actual dispersion relation, the one-dimensional (1D), $\omega = 2K\sin(aq/2)$, is used, leading to a change in frequencies

$$\omega' = \omega + \sqrt{1-(\omega/\omega_{\max})^2}\,\Delta\omega \tag{5}$$

with $\Delta\omega = Ka\Delta q$ and $\omega_{\max} = 2$ K. In a final step of approximation, this formula is applied for the disordered systems although the concept of a wave number q does not hold in this case.

Equation (5) now allows to rescale the reduced VDOS of the PBC system to that of the confined systems via

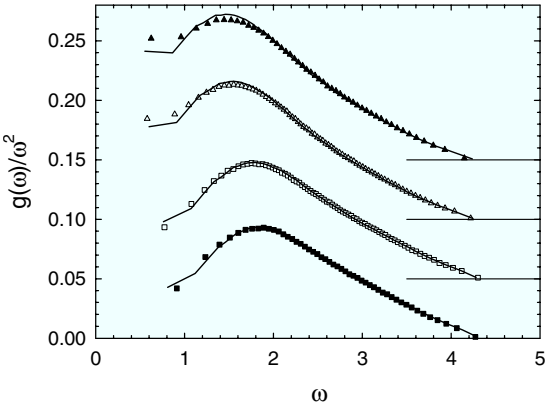

FIG. 9. Comparison of the simulated VDOS for the confined systems (symbols) with that of the PBC system rescaled by relations (6) and (5) (lines). From bottom to top, the systems are: $L=15$ hard (filled squares), $L=23$ hard (empty squares), $L=23$ soft (empty triangles), and $L=15$ soft (filled triangles). To avoid overlap, the curves are vertically shifted by 0.05 from system to system.

$$\frac{g'(\omega')}{\omega'^2} = \left(\frac{\omega}{\omega'}\right)^2 \frac{\mathrm{d}\omega}{\mathrm{d}\omega'} \frac{g(\omega)}{\omega^2} \tag{6}$$

with ω' inserted from (5).

B. Test on the numerical model

Figure 9 shows a fit of the rescaled VDOS to the actual numerical results from the confined systems. $\Delta\omega$ and $\omega_{\max}$ are treated as fit parameters (see Table III). The frequency offset resulting from Eq. (5) for these parameters is also what is shown as continuous curve in Fig. 8.

Considering the rough approximations used and the deviations visible in Fig. 8, the rescaling formula works surprisingly well for the VDOS. The soft confined systems are not described as well as the hard in the low-frequency region. This can be understood by the fact that Eq. (5) for $\Delta\omega < 0$ implies a reduction of ω' also for the lowest ω (even resulting in negative values), which is not present in the real transition PBC-soft for the (0,0,0) mode.

It is worth mentioning in which term of Eq. (6) the difference of the VDOS between confined and bulk systems is primarily rooted: the shift ($\Delta\omega = \pm 0.123$) of frequencies is nearly invisible on the whole ω scale. Also the differential $\mathrm{d}\omega/\mathrm{d}\omega'$ is close to one. The term causing the large differences in the low-frequency region is $(\omega/\omega')^2$ because for low frequencies, the small difference between ω' and ω has a large effect. Therefore, the difference in the VDOS is better

TABLE III. Parameters used in Eq. (5) to obtain the fits shown in Fig. 9.

L	Confinement type	$\Delta\omega$	$\omega_{\max}$
15	Hard	$+0.123 \pm 0.003$	4.5 ± 0.2
23	Hard	$+0.084 \pm 0.002$	4.5 ± 0.3
23	Soft	-0.083 ± 0.002	4.27 ± 0.08
15	Soft	-0.123 ± 0.004	4.27 ± 0.03

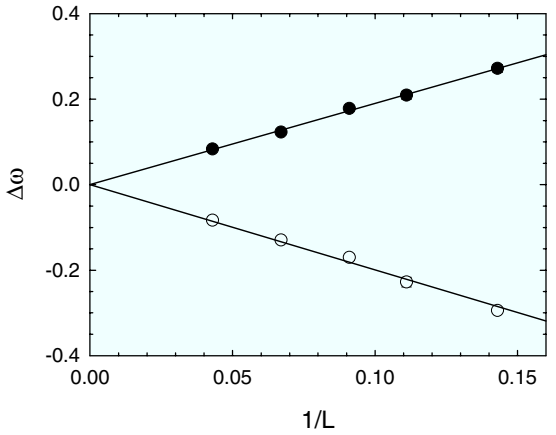

FIG. 10. Plot of $\Delta\omega$ from rescaling fits to confined systems of different size. Filled symbols correspond to hard confinement and empty symbols to soft confinement. The lines are fits of proportionalities $\Delta\omega \propto 1/L$.

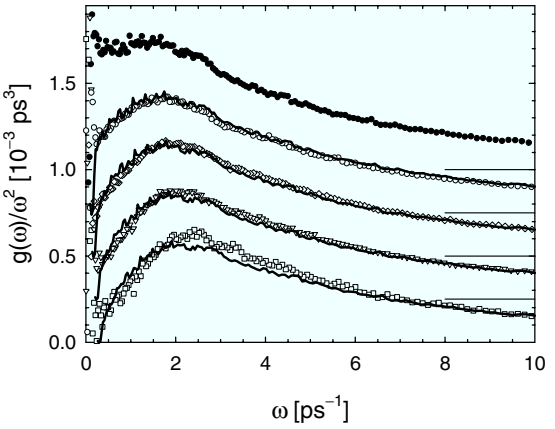

FIG. 11. Reduced VDOS of salol confined in nanoporous silica and of bulk salol. From bottom to top the systems are: confined 25 Å (squares), 50 Å (triangles), 75 Å (diamonds), 200 Å (hollow circles), and bulk (filled circles). To avoid overlap, the data are vertically shifted by 0.25×10^{-3} ps^3 from system to system. The lines result from rescaling the bulk VDOS (topmost data set, filled circles) using Eqs. (6) and (5) with $\omega_{max}=\infty$ and $\Delta\omega$ from Table IV.

visible in the "reduced representation" $g(\omega)/\omega^2$, which is usually done to show the BP. If $g(\omega)$ is plotted, the difference is much less prominent and may be overlooked.

There is no way to calculate the exact value of $\Delta\omega$ in relation (5), therefore it was treated as a fit parameter. Nevertheless, one would expect a certain scaling of $\Delta\omega$ with the size L for otherwise identical systems: in the ordered systems, the shift in eigenfrequencies results from a change in the components of some mode index components k_α by $\pm1/2$, independent of the size. If these changes occur with the same frequentness for systems of different size one, would expect the effective change in the wave number to scale as $\Delta q=(2\pi/La)\Delta k\propto 1/L$. Consequently, the scaling for the lower limit of the eigenfrequency offset should be $\Delta\omega \propto 1/L$ too. This relation is checked in Fig. 10 where the fit parameter $\Delta\omega$ is plotted vs $1/L$ for hard- and soft-confined systems of different size. It can be seen that the expected scaling relation with system size is excellently fulfilled.

The arguments used to derive relation (5) are also valid for systems confined only in one or two dimensions with the only difference that the number of mode indices shifted by $\pm1/2$ due to the confined boundary conditions is smaller. Therefore, the rescaling with relation (5) is possible for the partially confined systems too (fits in Fig. 3). A deeper analysis shows that the number of shifted modes is proportional to the number of confined dimensions D_{conf} in the ordered system. In consequence, one would expect $\Delta q\propto D_{conf}$ and for the disordered system $\Delta\omega\propto D_{conf}$. As the inset in Fig. 3 demonstrates, this proportionality is also fulfilled.

On the same grounds the, "compensation effect" of hard and soft surfaces (Fig. 4) is not surprising: the eigenmodes of the corresponding ordered system in the notation of Eq. (4) have $k_\alpha=(2n-1)/4$ with integer $n\geq1$ in the spatial direction(s) α, which is/are "mixed-confined." So there is always one mode reduced by $-1/4$ and one increased by $+1/4$ corresponding to the sine and cosine modes of the PBC system. The two opposite shifts lead to an unchanged average mode density.

C. Test on real systems

The validity of the rescaling procedure can also be tested for real confined glasses. VDOS data was obtained by INS from the organic glass-former salol in nanoporous silica in Ref. 34. Figure 11 shows a comparison of the actual VDOS in the confined systems with the rescaled VDOS of the bulk. Because ω_{max} does not significantly influence the scaling for low ω, it was set to infinity effectively reducing expression (5) to $\omega'=\omega+\Delta\omega$, and only $\Delta\omega$ was fitted here. The resulting values are shown in Table IV. Considering that in the real systems there is structural disorder in addition, and thus another premise of Eq. (5) is not fulfilled, the agreement is remarkably good.

Nevertheless, two shortcomings have to be mentioned: (i) the agreement progressively worsens for smaller confinement size. This may be due to a larger (relative) polydispersity for the small pores. (ii) $\Delta\omega$ is expected to be inverse proportional to the system size (as shown for the numerical model systems in Fig. 10). The ratio of the confinement sizes here leads to an expected ratio of 8 between the confinement sizes 25 and 200 Å; instead, the fit yields $\Delta\omega(25\text{ Å})=(0.241\pm0.006)$ ps^{-1} and $\Delta\omega(200\text{ Å})=(0.076\pm0.001)$ ps^{-1} with a ratio of 3.2 only. This lack of the expected system-size scaling was already noticed in Ref. 34 from a simple sound wave picture.

TABLE IV. Values of $\Delta\omega$ used to rescale the bulk VDOS to the VDOS in confinement in Fig. 11.

Confinement size [Å]	$\Delta\omega$ [ps^{-1}]
25	0.241 ± 0.006
50	0.182 ± 0.004
75	0.119 ± 0.002
200	0.076 ± 0.001

V. CONCLUSIONS

In summary, it could be shown that the model of a crystalline structure with force-constant disorder[9,16] reproduces the experimentally observed confinement effect on the boson peak (BP) when nonperiodic boundary conditions are introduced. The maximum of the BP is shifted to higher frequencies and the vibration density of states (VDOS) below the BP is reduced for hard confinement, realized by rigid boundary conditions (in comparison to periodic boundary conditions). Soft confinement, realized by open boundary conditions, has the opposite effect. The similarity between model and real amorphous systems strengthens the point that the maximum in the reduced VDOS observed in the disordered force-constant model indeed corresponds to the BP observed in experiments on structurally disordered materials.

The strength of the effect is proportional to the dimensionality of the confinement and inverse proportional to its size. Also, there is a compensation of hard and soft surfaces. No fundamental change in the localization properties (level statistics and participation ratio) due to confinement was observed. There is also no significant difference of the sound velocity induced by the variation of the boundary conditions. Nevertheless, the low-frequency limit of the VDOS *is* affected. The reason for this seeming contradiction is that the homogenous distribution of modes in reciprocal space, which is required for the Debye model, is significantly disturbed by nonperiodic boundary conditions.

The model offers as explanation of the confinement effect that the vibrational eigenfrequencies are shifted to higher values for boundary conditions corresponding to hard confinement and to lower values for soft confinement. Inspection of the corresponding force-ordered crystalline systems reveals as underlying reason that the modes, which are not allowed due to the "confinement" boundary conditions "evade" to higher or lower frequency for hard and soft confinement, respectively.

A common way to explain confinement effects in glass-forming materials is to postulate a cooperativity length scale, which is cut off by the confinement size.[35] For the model systems studied here, this explanation can be ruled out because the effect on the BP occurs only if the boundary conditions are changed and not just by a change in the size of the periodic boundary conditions (PBC) system. Another explanation suggested earlier was the suppression of surface modes close to the confinement boundary.[36] As there is no change in the general localization properties, this also seems not to be applicable here.

The overall change in eigenfrequencies by modification of the boundary conditions can be expressed by a simple relation, Eq. (5). From this, a rescaling of the VDOS can be derived, which works well for the numerical model systems. It is also applicable to the VDOS of real experimental systems, but there the agreement is less precise and the size scaling not fulfilled. The reason for this may be the imperfect realization of the confinement size and shape in the experiment. But the qualitative agreement is an indication that confinement of effect of the BP of real systems is of the same nature. A crucial experiment would be to look for the "compensation" (Fig. 4) in extremely thin films of less than 5 nm thickness.

ACKNOWLEDGMENT

I wish to thank U. Buchenau for critical reading of the article and helpful suggestions.

[1] Amorphous Solids, in *Low-Temperature Properties*, edited by W. A. Phillips (Springer, Berlin, 1981).
[2] R. C. Zeller and R. O. Pohl, Phys. Rev. B **4**, 2029 (1971).
[3] R. H. Stolen, Phys. Chem. Glasses **11**, 83 (1970).
[4] U. Buchenau, N. Nücker, and A. J. Dianoux, Phys. Rev. Lett. **53**, 2316 (1984).
[5] A. I. Chumakov, I. Sergueev, U. van Bürck, W. Schirmacher, T. Asthalter, R. Rüffer, O. Leupold, and W. Petry, Phys. Rev. Lett. **92**, 245508 (2004).
[6] V. G. Karpov, M. I. Klinger, and F. N. Ignatiev, Sov. Phys. JETP **57**, 439 (1983).
[7] U. Buchenau, Yu. M. Galperin, V. L. Gurevich, D. A. Parshin, M. A. Ramos, and H. R. Schober, Phys. Rev. B **46**, 2798 (1992).
[8] W. Schirmacher and M. Wagener, in *Dynamics of Disordered Materials*, Springer Proceedings in Physics Vol. 37, edited by D. Richter, A. J. Dianoux, W. Petry, and J. Teixeira (Springer, Heidelberg, 1989), p. 231.
[9] S. N. Taraskin, Y. L. Loh, G. Natarajan, and S. R. Elliott, Phys. Rev. Lett. **86**, 1255 (2001).
[10] R. Zorn, D. Richter, L. Hartmann, F. Kremer, and B. Frick, J. Phys. IV **10**, Pr7-83 (2000).
[11] B. Frick, C. Alba-Simionesco, G. Dosseh, C. Le Quellec, A. Moreno, J. Colmenero, A. Schönhals, R. Zorn, K. Chrissopoulou, S. Anastasiadis, K. Dalnoki-Verres, and A. Higgins, J. Non-Cryst. Solids **351**, 2657 (2005).
[12] T. Asthalter, M. Bauer, U. van Bürck, I. Sergueev, H. Franz, and A. I. Chumakov, Eur. Phys. J. E **12**, S9 (2003).
[13] C. Alba-Simionesco, G. Dosseh, E. Dumont, B. Frick, B. Geil, D. Morineau, V. Teboul, and Y. Xia, Eur. Phys. J. E **12**, 19 (2003).
[14] L.-M. Wang, F. He, and R. Richert, Phys. Rev. Lett. **92**, 095701 (2004).
[15] R. Zorn, M. Mayorova, D. Richter, and B. Frick, Soft Matter **4**, 522 (2008).
[16] W. Schirmacher, G. Diezemann, and C. Ganter, Phys. Rev. Lett. **81**, 136 (1998).
[17] H. R. Schober, J. Phys.: Condens. Matter **16**, S2659 (2004).
[18] A. Tanguy, J. P. Wittmer, F. Léonforte, and J.-L. Barrat, Phys. Rev. B **66**, 174205 (2002).
[19] F. Finkemeier and W. vonNiessen, Phys. Rev. B **63**, 235204 (2001).
[20] F. Léonforte, A. Tanguy, J. P. Wittmer, and J.-L. Barrat, Phys. Rev. Lett. **97**, 055501 (2006).
[21] J. K. Christie, S. N. Taraskin, and S. R. Elliott, J. Non-Cryst. Solids **353**, 2272 (2007).
[22] J. K. Christie, S. N. Taraskin, and S. R. Elliott, Phys. Status

Solidi C **1**, 2904 (2004).
[23] A particularity of the simple-cubic lattice is that for (more realistic) vectorial displacements the three space directions decouple in harmonic approximation. The Hamiltonian matrix can be decomposed into three independent matrices describing the motions in the Cartesian directions. Therefore, the vectorial treatment of the vibrations would not change the result except for an improvement of the statistics by a factor of three.
[24] R. J. Bell, N. F. Bird, and P. Dean, J. Phys. C **1**, 299 (1968).
[25] R. Zorn, M. Mayorova, D. Richter, A. Schönhals, L. Hartmann, F. Kremer, and B. Frick, AIP Conf. Proc. **982**, 79 (2008).
[26] D. Fioretto, U. Buchenau, L. Comez, A. Sokolov, C. Masciovecchio, A. Mermet, G. Ruocco, F. Sette, L. Willner, B. Frick, D. Richter, and L. Verdini, Phys. Rev. E **59**, 4470 (1999).
[27] C. B. Roth and J. R. Dutcher, J. Electroanal. Chem. **584**, 13 (2005); J. A. Forrest and K. Dalnoki-Verres, Adv. Colloid Interface Sci. **94**, 167 (2001).
[28] B. Frick, K. Dalnoki-Verres, J. A. Forrest, J. Dutcher, C. Murray, and A. Higgins, Eur. Phys. J. E **12**, S93 (2003).
[29] K. Fukao, S. B. Uno, Y. Miyamoto, Y. Hoshino, and H. Miyaji, J. Non-Cryst. Solids **307-310**, 517 (2002).
[30] R. Inoue, T. Kanaya, K. Nishida, I. Tsukushi, and K. Shibata, Phys. Rev. Lett. **95**, 056102 (2005); Phys. Rev. E **74**, 021801 (2006).
[31] H. R. Schober and C. Oligschleger, Phys. Rev. B **53**, 11469 (1996).
[32] S. N. Taraskin, J. J. Ludlam, G. Natarajan, and S. R. Elliott, Philos. Mag. B **82**, 197 (2002).
[33] If $k_\alpha=0$, the corresponding trigonometric function can only be a sine. With this restriction, the numbering scheme gives L^3 modes as required.
[34] R. Zorn, B. Frick, L. Hartmann, F. Kremer, A. Schönhals, and D. Richter, Physica B **350**, e1115 (2004).
[35] M. Arndt, R. Stannarius, H. Groothues, E. Hempel, and F. Kremer, Phys. Rev. Lett. **79**, 2077 (1997).
[36] R. Zorn, L. Hartmann, B. Frick, D. Richter, and F. Kremer, J. Non-Cryst. Solids **307-310**, 547 (2002).